Desalination and Water Treatment
www.deswater.com

doi: 10.1080/19443994.2016.1146166

57 (2016) 23536–23545
October

Taylor & Francis
Taylor & Francis Group

Effects of processing parameters on the pore structure of mesoporous carbon membranes

Guotong Qin[a], Hua Wen[a], Wei Wei[b,*]

[a]*Key Laboratory of Bio-Inspired Smart Interfacial Science and Technology of Ministry of Education, School of Chemistry and Environment, Beihang University, 37 Xueyuan Road, Beijing 100191, China, Tel. +86 10 82338556; emails: qingt@buaa.edu.cn (G. Qin), 415905311@qq.com (H. Wen)*
[b]*College of Arts and Science, Beijing Union University, 197 Beituchengxi Road, Beijing 100191, China, Tel./Fax: +86 10 62004523; emails: wlweiwei@buu.edu.cn, weiwei@ygi.edu.cn*

Received 27 June 2015; Accepted 28 December 2015

ABSTRACT

Mesoporous carbon membranes have been prepared by means of an organic sol–gel method. The sol formed by resorcinol and formaldehyde was layered on the outer surface of a fly-ash-based microfiltration ceramic membrane, and was then subjected to gelling, drying, and carbonization to form a mesoporous carbon layer. Several surfactants were used to allow the carbon membranes to dry under ambient pressure. The pore properties of the carbon membranes have been examined by physical adsorption of nitrogen and subsequent pore structure analysis. The surface area, mesopore volume, and average pore diameter have been controlled by changing the surfactant species and concentration, the resorcinol/formaldehyde concentration, and the sol synthesis time. The as-prepared carbon membranes showed high performance with low transport resistance. The pore size/distribution can be tailored for a specific separation process by adjusting the preparation conditions. These carbon membranes can be applied in ultrafiltration separation processes.

Keywords: Mesoporous carbon membrane; Sol–gel polymerization; Preparation; Nitrogen adsorption; Pore structure

1. Introduction

Carbon membranes can be applied in gas separation, ultrafiltration, and microfiltration according to their pore structure. They are produced by pyrolyzing different polymeric materials. The pore structure of the membrane can be determined by precursors and preparation conditions. Many researches focus on the preparation of microporous carbon membranes for gas separation [1–6]. Carbon membranes for gas separation have a narrow range of microporosity (0.3–1 nm), which allows discrimination between gas molecules of different sizes. The research about mesoporous carbon membranes with average pore diameters of 1–100 nm for ultrafiltration is few. Sachdeva and Kumar [7] prepared a carbon membrane with an average pore diameter of 1.8 nm; this membrane could separate basic dyes such as rhodamine B with a rejection range 90–100%. Shah et al. [8] prepared a carbon membrane with a mean pore diameter of 12.3 nm, which could be employed for protein ultrafiltration. The sol–gel method is a route to prepare mesoporous

---

*Corresponding author.

carbon membranes. Yoshimune et al. [9] prepared freestanding mesoporous carbon membranes by a sol–gel process using resorcinol and formaldehyde. Mesoporous polymer membranes were first washed three times with *t*-butanol and freeze-dried at 263 K. The polymer membranes were then carbonized at 950℃ to produce mesoporous carbon membranes with pore diameters of 5.48 nm and 13.9 nm. Their permeance to He was about $5–15 \times 10^{-7}$ mol m^{-2} s^{-1} Pa^{-1}. Shih-Hong Hsu et al. [10] coated a mesoporous carbon aerogel on a macroporous alumina tubular support to form a tubular carbon aerogel membrane by a sol–gel process. The preparation process involved an ethanol wash. The carbon membrane was obtained after carbonization at 1,273 K for 6 h. The thickness and average pore diameter of the carbon aerogel membrane was approximately 10 μm and 10 nm, respectively. The disadvantage of this method is that it needs a high-volume solvent wash and a special drying process such as supercritical drying or freeze-drying, expensive and risky. Many researchers studied the novel methods to simplify the drying process. Bruno et al. [11,12] used cationic polyelectrolyte as stabilizer to prepared bulk resorcinol–formaldehyde (RF) aerogels and carbon aerogels. Ambient drying was employed instead of complex drying process which significantly simplified the process and saved energy. Later, Balach et al. [13] tailored the pore size by changing the concentration of the polyelectrolyte using ambient drying.

In our previous work [14], we prepared a supported mesoporous carbon membrane by sol–gel method using ambient drying. The advantage of this method is that the preparation process is simple without a high-volume solvent wash and special drying method. However, the obtained carbon membranes showed poor permeation performance. It has been found that crucial aspects in the preparation of these carbon membranes are the processing conditions. Therefore, it is very important to find out how the processing parameters affect the pore structure of carbon membranes. The objective of the current study is to develop high-quality mesoporous carbon membranes using different surfactants. The effects of the processing parameters, such as surfactant species and concentration, RF concentration, and sol synthesis time, on the pore structure of the membranes were systematically investigated.

2. Experimental

2.1. Synthesis of RF sols

Three ionic surfactants (sodium dodecylsulfonate, tetrabutylammonium bromide, and cetyl trimethylammonium bromide) were used to synthesize RF sols, respectively. All of these surfactants were also served as basic catalysts (C). After the formaldehyde and resorcinol were dissolved in water, these surfactants were added, respectively. The solutions were poured into the glass vials, which were then sealed and immersed in a thermostated water bath at 42℃. The initially clear solutions slowly became white and opaque. The viscosity of the reacting sol increased rapidly, indicating a sol–gel transition. The R/F molar ratio was maintained at 0.5. The RF concentration, R/C molar ratio, and sol synthesis time were varied.

2.2. Preparation of carbon membranes

We used homemade fly-ash-based microfiltration tubular ceramic membranes with an average pore size of 0.4 μm as supports. The microfiltration membrane is inexpensive and shows high permeability due to the shape of the raw material particles [15,16]. The gelation time was defined as the time elapsed when the sol no longer flowed, also called the sol–gel transition. Before gelation, we applied one coating of the sol on the supports, and then dried the coated supports at 42℃ in a desiccator saturated with formaldehyde. The coated supports were then heated to 150℃ at a rate of 0.5℃/min in air. Finally, the coated supports were heated to 800℃ at a rate of 2℃/min under a nitrogen

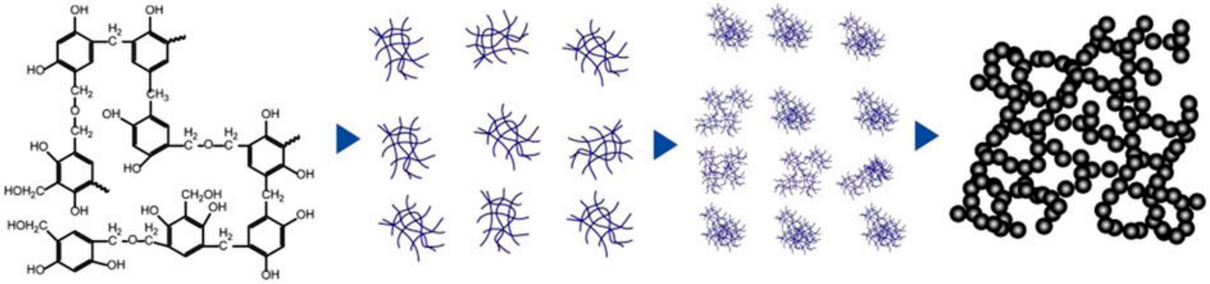

Fig. 1. Schematic diagram of the formation of mesoporous gel membrane.

atmosphere and were maintained at this temperature for 1 h. Mesoporous carbon membranes were thereby obtained.

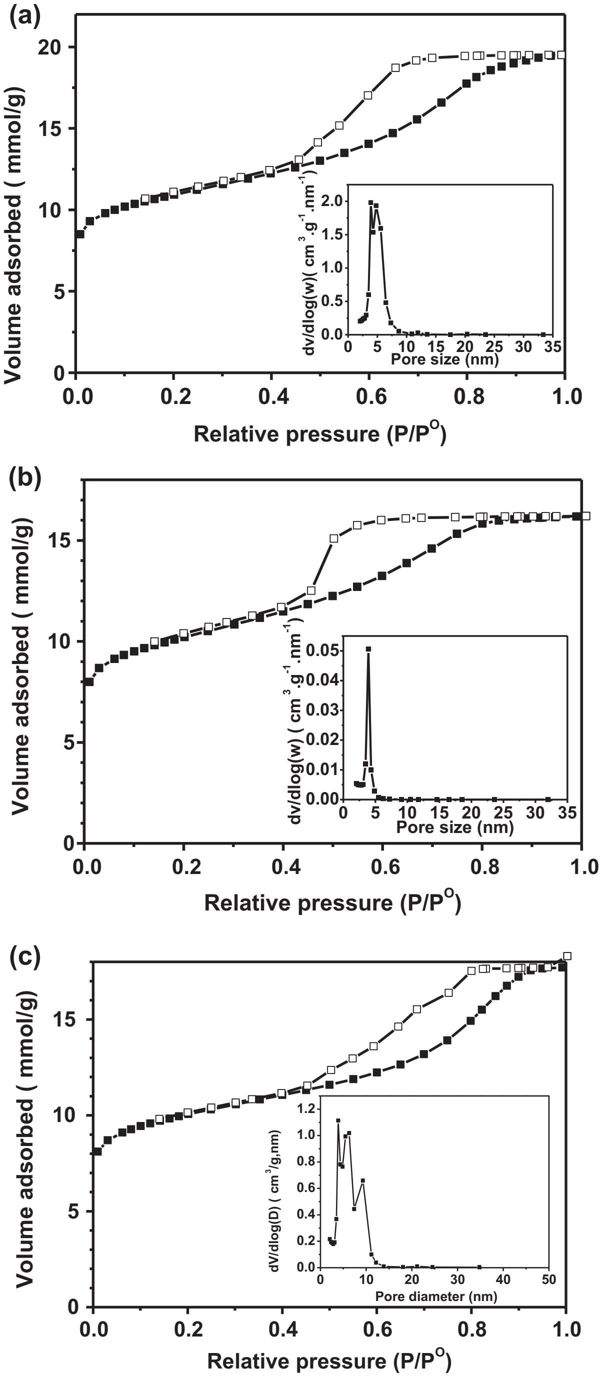

Fig. 2. Adsorption profiles of N_2 and pore size distributions (inset images) of carbon membranes generated by different surfactants ((a) tetrabutyl ammonium bromide; (b) sodium dodecylsulfonate; (c) cetyl trimethyl ammonium bromide).

2.3. Characterization

Polymer and carbon films without supports were prepared similarly to those with supports. These samples were later ground into powder for adsorption experiments. Nitrogen adsorption measurements were carried out on a Micromeritics ASAP 2020 apparatus. The samples were degassed at 100℃ prior to the measurements. The surface areas and pore volumes of these samples were evaluated from their N_2 adsorption isotherms. The pore size distributions were calculated using the BJH (Barrett-Joyner-Halenda) theory from the desorption branch of the nitrogen isotherms. Pure gases (H_2, CO_2, N_2, O_2, and Ar) were used to test the permeance and integrity of the carbon membrane. The flow rates of these gases through the carbon membrane were measured at 25℃ using a soap-film flowmeter or wet gas flowmeter. The carbon membrane area was 13.2 cm^2.

Permeances of the different gases were calculated from the expression:

$$J_{\mathrm{i}} = \frac{Q_{\mathrm{i}}}{\Delta P} \tag{1}$$

where J_{i} is the permeance (mol m^{-2} s^{-1} Pa^{-1}) of species i, Q_{i} is the gas flux (mol m^{-2} s^{-1}), and ΔP is the pressure difference (Pa).

Scanning electron microscopy (SEM) images were acquired with an FEI Quanta FEG$^{\mathrm{TM}}$ 250 scanning electron microscope (FEI Company, USA).

3. Results and discussion

3.1. Surfactant species and concentration

The preparation of the carbon membranes involved three stages. In the first stage, the sol was prepared in a sealed glass vial. The sol was then coated on the support and formed a wet gel membrane. In the second stage, the gel membrane was dried. In the third stage, the dried membrane was carbonized. Fig. 1 shows the formation of mesoporous gel membrane. The clusters formed and grew during sol synthesis. During gelation, the clusters connected with each other and formed pores. Then the pores shrank through drying and carbonization.

Generally, a special drying process such as freeze-drying or supercritical drying is needed to avoid pore collapse caused by capillary pressure built up in the pore walls of the organic gel membrane. In this study, surfactant molecules absorbed on the surfaces of the RF sols formed microemulsions, which eventually lowered the surface tension at the water–resin interface in

Table 1
Characteristics of gel membranes and carbon membranes by different surfactants

Surfactants	Membrane	S_{BET} ($m^2\ g^{-1}$)	V_{meso} ($cm^3\ g^{-1}$)	V_{micro} ($cm^3\ g^{-1}$)	Mean pore diameter (nm)
$C_{19}H_{42}BrN$	Gel	113	0.19	0.00	6.8
	Carbon	770	0.42	0.21	4.9
$C_{12}H_{25}NaO_3S$	Gel	262	0.37	0.01	4.8
	Carbon	785	0.40	0.20	3.6
$C_{16}H_{36}BrN$	Gel	273	0.37	0.01	4.5
	Carbon	784	0.50	0.22	4.3

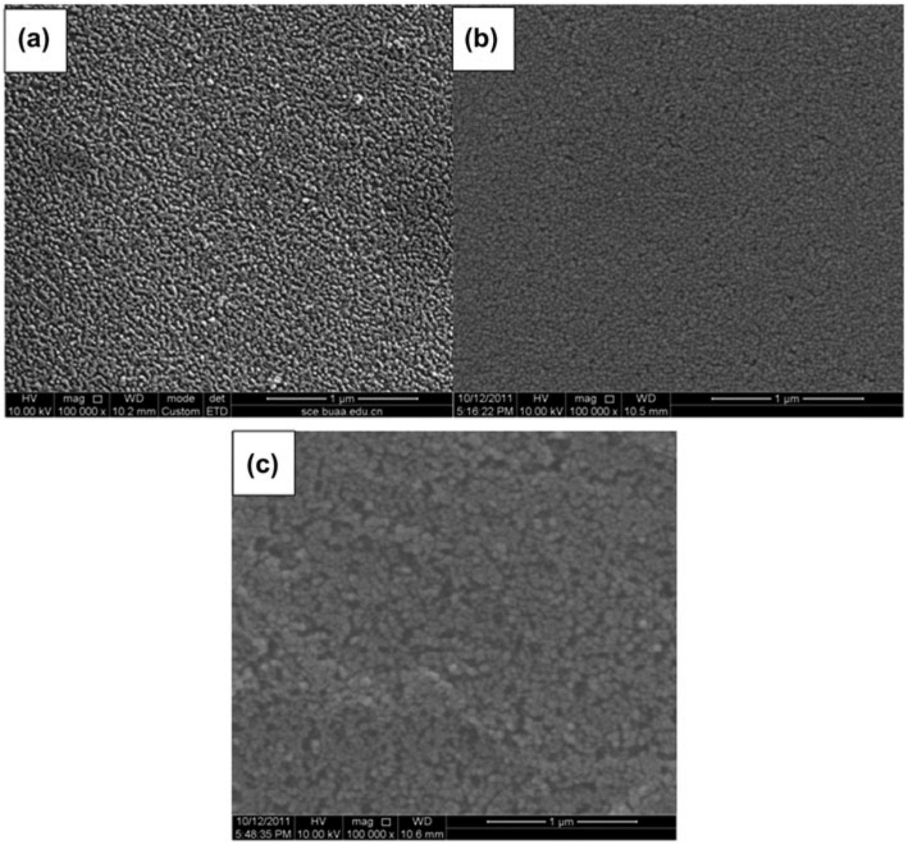

Fig. 3. SEM micrographs of the surface of carbon membranes synthesized by different surfactants ((a) tetrabutyl ammonium bromide; (b) sodium dodecylsulfonate; (c) cetyl trimethyl ammonium bromide), the scale bar 1 micron.

the pores [17]. Additionally, the coated supports were dried in a desiccator saturated with formaldehyde, which prevented significant shrinkage and maintained the mesoporous structure of the membranes. In this way, the gel membranes could be dried at ambient pressure without a special drying process. Considering the consumption of the surfactant and the size of micelle the selected surfactants should have a low/medium molecular weight. The polymerization of resorcinol with formaldehyde needs basic catalyst. Therefore, we chose sodium dodecylsulfonate, tetrabutylammonium bromide, and cetyl trimethylammonium bromide as surfactants. The RF concentration was 20%, R/C molar ratio was 200, and the sol synthesis time was about 90% of the gelation time. Fig. 2 shows the adsorption and desorption isotherms of N_2 at 77 K and the pore size distributions of carbon membranes synthesized with three surfactants. Three carbon membranes exhibited type IV N_2 sorption isotherms. Considerable capillary condensation steps at

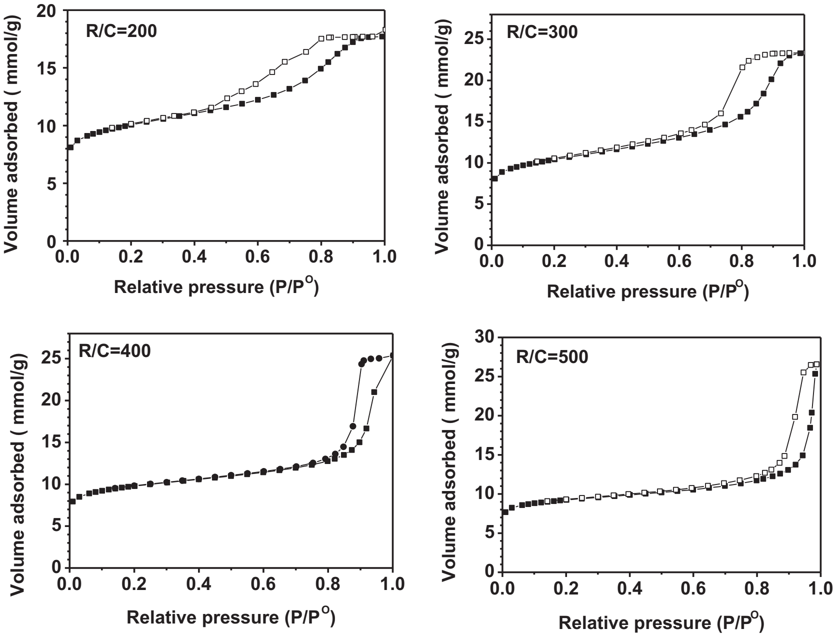

Fig. 4. Adsorption profiles of N_2 on carbon membranes generated by different R/C mole ratios.

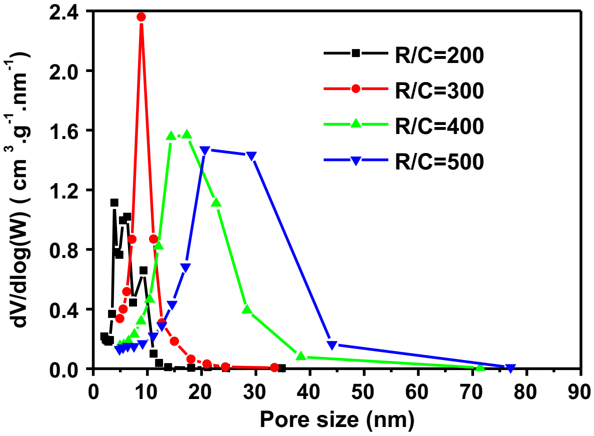

Fig. 5. Pore size distributions of carbon membranes generated by different R/C mole ratio.

relative pressures from 0.4 to 1.0 suggest well-developed mesoporosity. The pore size distribution plots indicate uniform mesopores in these membranes. The majority of the pores were smaller than 10 nm. The mean pore diameters of carbon membranes synthesized with sodium dodecylsulfonate, tetrabutylammonium bromide, and cetyl trimethylammonium bromide were 3.6, 4.3, and 4.9 nm, respectively.

Table 1 shows the characteristics of the gel membranes and carbon membranes synthesized with different surfactant species. The gel membranes were mesoporous with few micropores. The mesopore volume was 0.19–0.37 $cm^3\ g^{-1}$ and the micropore volume was below 0.01 $cm^3\ g^{-1}$. The micropores in the carbon membranes formed during the pyrolysis step. Gases such as H_2, CO_2, and CH_4 channeled through the membranes during pyrolysis, creating micropores. After pyrolysis, the micropore volume increased to around 0.20 $m^3\ g^{-1}$ and the mesopore volume increased to 0.40–0.50 $m^3\ g^{-1}$ due to weight loss of gel skeleton.

The BET surface area increased after carbonization, partly because of micropore formation. A shift toward smaller pore diameters, caused by the pyrolysis procedure, is also evident from Table 1.

Fig. 3 shows SEM images of carbon membrane surfaces synthesized using different surfactants. These carbon membranes were composed of carbon particle clusters with diameters of several tens of nanometers. Pores in these carbon membranes were formed by fissures and voids between the pure carbon particles. These micrographs show the presence of pores with nanometer-scale diameters. The results demonstrate that all three surfactants are appropriate for preparing mesoporous carbon membranes.

The surfactant molecules adsorbed on the intermediates forming a microemulsion during the sol–gel process. This microemulsion dispersed the intermediates, hampering their aggregation, which would otherwise have led to clusters in the micrometer range. Therefore, the microstructure of the carbon

Table 2
Effects of *R/C* on structure characteristics of gel membranes and carbon membranes by cetyl trimethyl ammonium bromide

R/C	Membrane	S_{BET} ($m^2 g^{-1}$)	V_{micro} ($cm^3 g^{-1}$)	V_{meso} ($cm^3 g^{-1}$)	Mean pore diameter (nm)
200	Gel	113	0.00	0.19	6.8
	Carbon	770	0.21	0.42	4.9
300	Gel	138	0.01	0.38	10.1
	Carbon	747	0.20	0.60	6.3
400	Gel	149	0.01	0.43	16.3
	Carbon	698	0.22	0.64	10.4
500	Gel	111	0.01	0.48	17.9
	Carbon	644	0.23	0.70	13.4

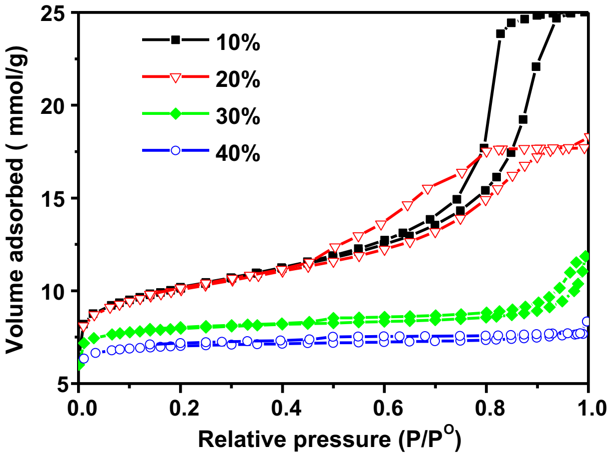

Fig. 6. Adsorption profiles of N_2 on carbon membranes generated by different RF concentrations.

membranes can be controlled by changing the surfactant concentration [18]. Figs. 4 and 5 show the adsorption and desorption isotherms of N_2 at 77 K and the pore size distributions of carbon membranes synthesized with cetyl trimethylammonium bromide at different R/C molar ratios. The adsorption volume increased with increasing R/C molar ratio. As the R/C molar ratio was increased, the pore diameter peak increased and the pore size distribution widened. Table 2 shows the effects of the R/C ratio on the structural characteristics of the gel membranes and carbon membranes. The mesopore volume and mean pore diameter increased as the R/C molar ratio was increased. An RF-based carbon membrane has a highly cross-linked structure of spherical particles. The mesopores in these membranes are voids between the interconnected particles. A higher surfactant concentration resulted in improved dispersion, which caused the particle sizes in the resultant network to be smaller. On the other hand, surfactants were also used as catalysts in this study. Decreased catalyst would yield looser cross-linking polymer particle, increasing the compatibility of RF polymer with solvents. The RF gels originated from a microphase separation, during which a transition occurred from nucleation-and-growth to spinodal decomposition. Increased compatibility resulted the polymer system persisted in longer time in the nucleation-and-growth regime and resulted larger particles [19]. The particle size increased with increasing R/C molar ratio [20]; thus, the pore size increased with the R/C molar ratio. The effects of the surfactant species on the pore structure of resultant carbon membranes might be related with the basic strength of the RF solution from different surfactants. In contrast to the mesopore volume, upon carbonization the micropore volume stayed nearly constant at 0.2 $cm^3 g^{-1}$ at varying R/C molar ratios. This behavior also demonstrates that the micropores were mainly formed during pyrolysis.

3.2. Effects of the RF concentration on carbon membrane characteristics

Figs. 6 and 7 show the nitrogen adsorption isotherms and pore size distributions of carbon membranes prepared with cetyl trimethylammonium bromide at different RF concentrations. Table 3 shows the pore structure characteristics of carbon membranes synthesized at different RF concentrations. The R/C ratio was maintained at 200. The sol synthesis time was 90% of the gelation time. All of the carbon membranes displayed type IV isotherms. The hysteresis observed in the N_2 adsorption/desorption isotherms can be attributed to the membrane mesoporosity. The amount of adsorption decreased with increasing RF concentration; the mesopore volume also decreased sharply. When the concentration was increased from

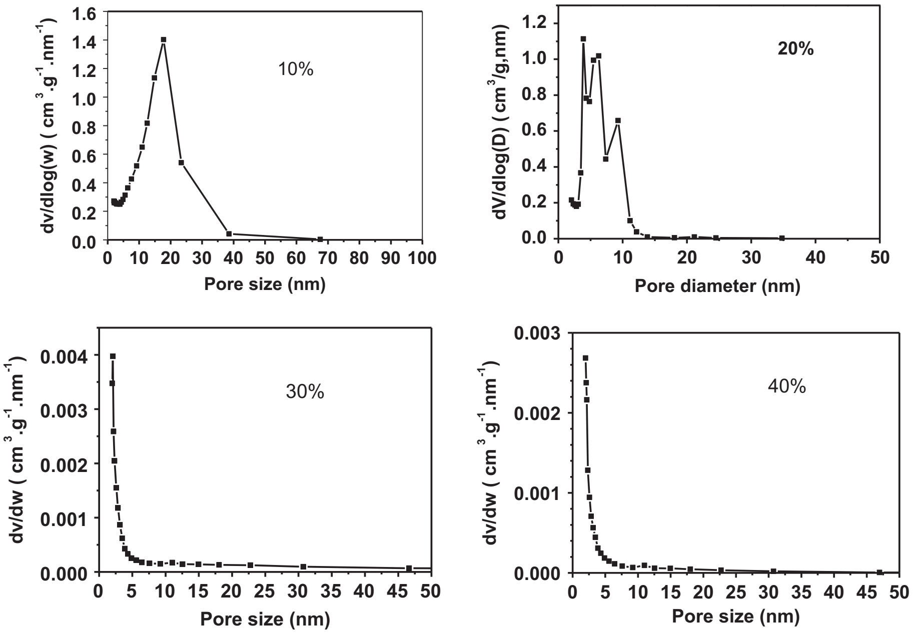

Fig. 7. Pore size distributions of carbon membranes generated by different RF concentrations.

Table 3
Effects of RF concentration on structure characteristics of carbon membranes

Concentration (%)	S_{BET} (m^2 g^{-1})	V_{micro} (cm^3 g^{-1})	V_{meso} (cm^3 g^{-1})	Mean pore size (nm)
10	720	0.22	0.68	7.8
20	770	0.21	0.42	4.9
30	541	0.23	0.16	5.9
40	474	0.21	0.06	5.4

10 to 40%, the mesopore volume decreased from 0.68 to 0.06 cm^3 g^{-1}. The mean pore diameter decreased from 7.8 to 5.4 nm.

The increase in the reactant concentration resulted in an increase in solid content in the sol and in the final gel. The fraction of solvent in the gel decreased accordingly. The mesopores originated from the shrunken voids due to evaporation of the solvent. The theoretical porosity is the fraction of the solvent in the sol, if we don't consider the shrinkage. Therefore, with an increase in reactant concentration the mesopore volume decreased.

Overall, a low RF concentration and high R/C ratio should be applied to obtain high-quality mesoporous carbon membranes.

3.3. *Effects of sol synthesis time on carbon membrane characteristics*

For the coating solution, we chose an RF sol prepared from cetyl trimethylammonium bromide (R/C = 400, RF concentration = 20%). The gelation time of this solution was about 23.5 h. Sol synthesis times of 14.5, 17, 19, and 21 h were chosen. It was difficult to peel the membrane from the support when the sol synthesis time was short. Therefore, a glass plate was used instead of the fly-ash-based ceramic support. Figs. 8 and 9 show the nitrogen adsorption isotherms and pore size distributions of the carbon membranes obtained from the sols with different synthesis times. Table 4 shows the effects of the sol synthesis time on the characteristics of the carbon membranes. The average pore diameter increased when the sol synthesis time was increased from 14.5 to 19 h. However, it barely changed when the sol synthesis time was further increased from 19 to 21 h. The mesopore volume and BET surface area decreased slightly as the sol synthesis time was increased. The characteristics of the carbon membrane prepared on the fly-ash-based ceramic support are also shown in Table 4. For a fixed sol synthesis time, the average pore diameter of a carbon membrane prepared on a

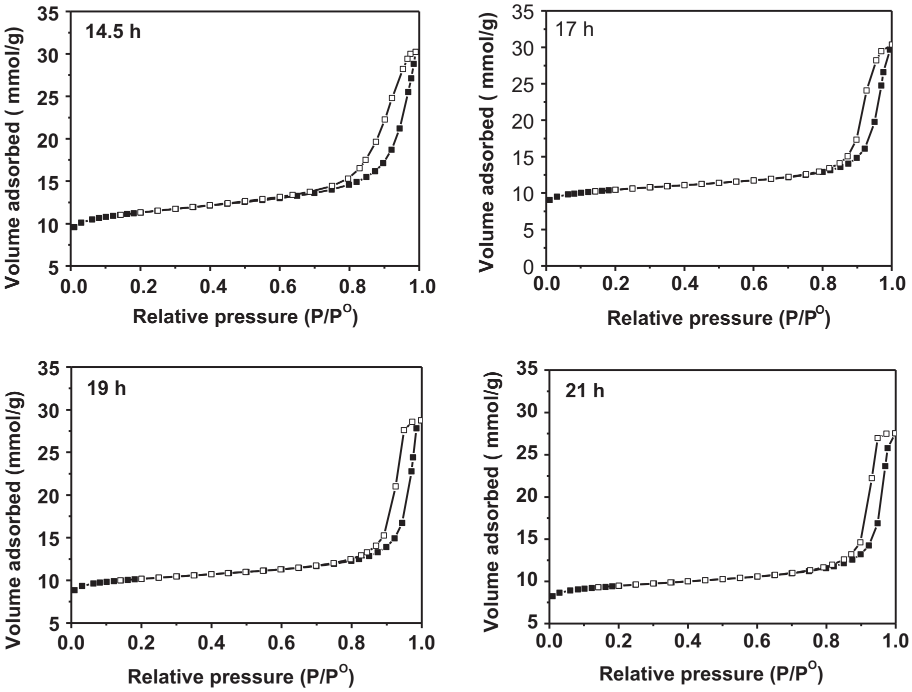

Fig. 8. Adsorption profiles of N_2 on carbon membranes generated by different sol synthesis times.

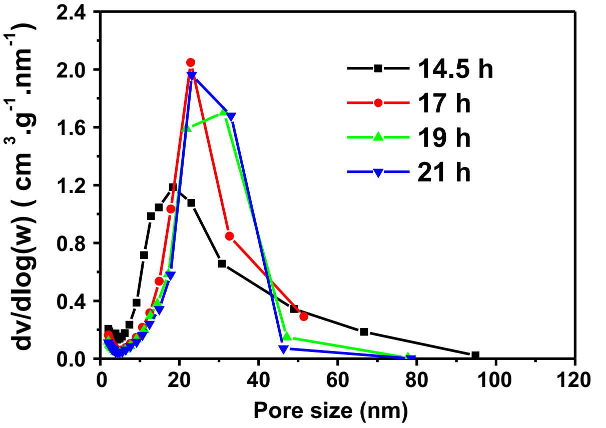

Fig. 9. Pore size distributions of carbon membranes generated by different sol synthesis times.

fly-ash-based ceramic support was smaller than that of the carbon membrane prepared on a glass plate.

At the beginning of the sol synthesis, few particles are present in the sol and the particle size is small. As the reaction proceeds, particles begin to form and grow up. The membrane mesopores are formed from the voids between the interconnected particles formed during gelation. Therefore, the pore size increased when the sol synthesis time was increased. However, as the gelation time approached, the particle size did not change, leading to no change in the pore size.

Increasing the sol synthesis time can thicken the membrane layer due to high viscosity. The thickness of the gel membrane is proportional to the root of the viscosity of the sol [21]. The gel membrane has to undergo a drying stress which is related with the thickness. Increased thickness will enhance the risk of cracking during drying. Furthermore, a thick separation layer also increases the cracking risk from carbonization due to thermal condensation. If the sol synthesis time is too short, several cycles of coating and pyrolysis must be performed to obtain a crack-free carbon membrane. Using multiple cycles also increases the membrane thickness and decreases the gas permeance. Therefore, applying an appropriate sol synthesis time can improve the membrane characteristics.

3.4. Membrane permeability

The R/C ratio, RF concentration, and sol synthesis time were fixed at 400, 20%, and 14.5 h, respectively. Fig. 10 shows the H_2, N_2, CO_2, O_2, and Ar permeances of the carbon membrane as a function of pressure at 25℃. The carbon membrane exhibited high fluxes for all of the gases tested, with typical gas permeances of $10^{-5} \times 10^{-6}$ mol m^{-2} s^{-1} Pa^{-1}, which are very high

Table 4
Effects of sol synthesis time on structure characteristics of carbon membranes

Sol synthesis time (h)	Supports	S_{BET} ($m^2 g^{-1}$)	V_{meso} ($cm^3 g^{-1}$)	V_{micro} ($cm^3 g^{-1}$)	Mean pore diameter (nm)
14.5	Glass	790	0.78	0.28	11.9
17	Glass	724	0.76	0.27	15.3
19	Glass	701	0.73	0.27	17.0
21	Glass	654	0.71	0.25	17.1
21	Fly-ash	698	0.64	0.22	10.4

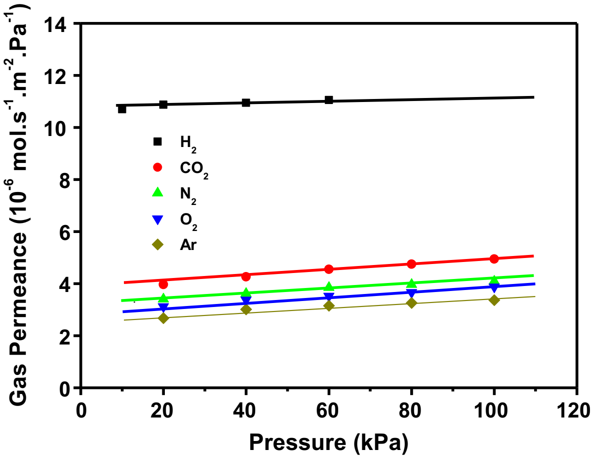

Fig. 10. Effects of pressure drop on gas permeance of the carbon membrane.

compared with other reported values [9,22–24]. Gas transport through the carbon membrane was found to be independent of the feed pressure on the whole. This implies that the prepared carbon membrane was crack-free and the pore sizes were nanometer scale.

For a membrane with a mean pore size between 1 and 100 nm, the average pore dimension can be estimated by examining data of the membrane gas permeability vs. the trans-membrane pressure [22]. The gas flux through the membrane can be written as:

Table 5
Pore sizes of the carbon membrane measured by different gases

Gas	Mean pore diameter (nm)	Mean value (nm)
H_2	14.20	8.04
CO_2	2.54	
N_2	6.76	
O_2	8.31	
Ar	8.37	

$$Q = \left(K_0 + \frac{B_0}{\eta}\bar{P}\right)\frac{\Delta P}{l} \quad (2)$$

where η is the gas viscosity (Pa s), $\bar{P}$ is the average trans-membrane pressure difference (Pa), and ΔP is the pressure driving force under gas permeation (Pa).

The structure factor B_0 is proportional to the square of the mean pore diameter:

$$B_0 = \frac{\varepsilon}{\tau^2\alpha}d_m^2 \quad (3)$$

with $\alpha = 2.5$ for consolidated media. The Knudsen permeability K_0 can be written as:

$$K_0 = \frac{4\beta\varepsilon}{3\tau^2\alpha}d_m\sqrt{\frac{8RT}{M}} \quad (4)$$

where $\beta = 0.8$ for consolidated media. Gas permeation data can be used to evaluate both B_0 and K_0. The ratio of these two parameters can be used to evaluate the mean pore diameter of the membrane d_m without any assumptions of the membrane porosity ε or tortuosity factor τ. Table 5 shows the mean pore diameters calculated by different gases using above formulas. The mean pore diameters were different when using different gases. The mean value was about 8.04 nm. The obtained carbon membrane can be used for ultrafiltration. The pure water flux and the molecular weight cut-off (determined by polyethylene glycol solutions) are about 156 L m^{-2} h^{-1} bar^{-1} and 17,000 Da.

4. Conclusion

Mesoporous crack-free carbon membranes have been prepared by a simple sol–gel method and carbonization. Gel membranes were dried at ambient pressure using surfactants to form a microemulsion, which decreased the surface tension. All three surfactants used (sodium dodecylsulfonate, tetrabutylammonium bromide, and cetyl trimethylammonium bromide) were appropriate for preparing such mesoporous carbon membranes. The carbon membranes were mesoporous with high mesopore volumes. Tuning the preparation conditions can control the membrane characteristics. The mesopore volume and average pore diameter increased with increasing R/C molar ratio. With increasing sol synthesis time, the mesopore volume and BET surface area decreased, while the average pore diameter increased. A high RF concentration resulted in a significant decrease in mesopore volume, which is undesirable when preparing mesoporous carbon membranes. Mesoporous carbon membranes with high permeance could be obtained by optimizing the preparation parameters.

Acknowledgments

Project 51172027 supported by NSFC.

References

[1] W. Wei, G. Qin, H. Hu, L. You, G. Chen, Preparation of supported carbon molecular sieve membrane from novolac phenol–formaldehyde resin, J. Membr. Sci. 303 (2007) 80–85.

[2] M.B. Shiflett, H.C. Foley, Ultrasonic deposition of high-selectivity nanoporous carbon membranes, Science 285 (1999) 1902–1905.

[3] M. Kiyono, P.J. Williams, W.J. Koros, Effect of pyrolysis atmosphere on separation performance of carbon molecular sieve membranes, J. Membr. Sci. 359 (2010) 2–10.

[4] S.M. Mahurin, J.S. Lee, X. Wang, S. Dai, Ammonia-activated mesoporous carbon membranes for gas separations, J. Membr. Sci. 368 (2011) 41–47.

[5] Z. Zhong, J. Yao, Z.-X. Low, R. Chen, M. He, H. Wang, Carbon composite membrane derived from a two-dimensional zeolitic imidazolate framework and its gas separation properties, Carbon 72 (2014) 242–249.

[6] X. Ning, W.J. Koyos, Carbon molecular sieve membranes derived from Matrimid (R) polyimide for nitrogen/methane separation, Carbon 66 (2014) 511–522.

[7] S. Sachdeva, A. Kumar, Preparation of nanoporous composite carbon membrane for separation of rhodamine B dye, J. Membr. Sci. 329 (2009) 2–10.

[8] T.N. Shah, H.C. Foley, A.L. Zydney, Development and characterization of nanoporous carbon membranes for protein ultrafiltration, J. Membr. Sci. 295 (2007) 40–49.

[9] M. Yoshimune, T. Yamamoto, M. Nakaiwa, K. Haraya, Preparation of highly mesoporous carbon membranes via a sol-gel process using resorcinol and formaldehyde, Carbon 46 (2008) 1031–1036.

[10] S.-H. Hsu, Y.-F. Lin, T.-W. Chung, T.-Y. Wei, S.-Y. Lu, K.-L. Tung, K.-T. Liu, Mesoporous carbon aerogel membrane for phospholipid removal from Jatropha curcas oil, Sep. Purif. Technol. 109 (2013) 129–134.

[11] M.M. Bruno, H.R. Corti, J. Balach, N.G. Cotella, C.A. Barbero, Hierarchical porous materials: Capillaries in nanoporous carbon, Funct. Mater. Lett. 2 (2009) 135–138.

[12] M.M. Bruno, N.G. Cotella, M.C. Miras, C.A. Barbero, A novel way to maintain resorcinol-formaldehyde porosity during drying: Stabilization of the sol-gel nanostructure using a cationic polyelectrolyte, Colloids Surf. A 362 (2010) 28–32.

[13] J. Balach, L. Tamborini, K. Sapag, D.F. Acevedo, C.A. Barbero, Facile preparation of hierarchical porous carbons with tailored pore size obtained using a cationic polyelectrolyte as a soft template, Colloids Surf. A 415 (2012) 343–348.

[14] G.T. Qin, C. Wang, W. Wei, Preparation of a mesoporous carbon membrane from resorcinol and formaldehyde, Carbon 48 (2010) 4206–4208.

[15] J. Fang, G.T. Qin, W. Wei, X.Q. Zhao, Preparation and characterization of tubular supported ceramic microfiltration membranes from fly ash, Sep. Purif. Technol. 80 (2011) 585–591.

[16] J. Fang, G.T. Qin, W. Wei, X.Q. Zhao, L. Jiang, Elaboration of new ceramic membrane from spherical fly ash for microfiltration of rigid particle suspension and oil-in-water emulsion, Desalination 311 (2013) 113–126.

[17] K.T. Lee, S.M. Oh, Novel synthesis of porous carbons with tunable pore size by surfactant-templated sol-gel process and carbonisation, Chem. Commun. 22 (2002) 2722–2723.

[18] D.C. Wu, R.W. Fu, M.S. Dresselhaus, G. Dresselhaus, Fabrication and nano-structure control of carbon aerogels via a microemulsion-templated sol-gel polymerization method, Carbon 44 (2006) 675–681.

[19] D.W. Schaefer, R.W. Pekala, G. Beaucage, Origin of porosity in resorcinol-formaldehyde aerogels, J. Non-Cryst. Solids 186 (1995) 159–167.

[20] G.C. Ruben, R.W. Pekala, T.M. Tillotson, L.W. Hrubesh, Imaging aerogels at the molecular level, J. Mat. Sci. 27 (1992) 4341–4349.

[21] C.J. Brinker, A.J. Hurd, P.R. Schunk, G.C. Frye, C.S. Ashley, Review of sol-gel thin film formation, J. Non-Cryst. Solids 147&148 (1992) 424–436.

[22] M.S. Strano, A.L. Zydney, H. Barth, G. Wooler, H. Agarwal, H.C. Foley, Ultrafiltration membrane synthesis by nanoscale templating of porous carbon, J. Membr. Sci. 198 (2002) 173–186.

[23] X.Q. Wang, Q. Zhu, S.M. Mahurin, C.D. Liang, S. Dai, Preparation of free-standing high quality mesoporous carbon membranes, Carbon 48 (2010) 557–560.

[24] S. Tanaka, N. Nakatani, A. Doi, Y. Miyake, Preparation of ordered mesoporous carbon membranes by a soft-templating method, Carbon 49 (2011) 3184–3189.